

## Studies on gas sensing performance of pure and modified barium strontium titanate thick film resistors

G H JAIN, L A PATIL\*, P P PATIL<sup>†</sup>, U P MULIK<sup>††</sup> and K R PATIL<sup>#</sup>

P.G. Department of Physics, Pratap College, Amalner 425 401, India

<sup>†</sup>Physical Sciences, North Maharashtra University, Jalgaon 425 001, India

<sup>††</sup>Centre for Materials for Electronics Technology, Pune 411 008, India

<sup>#</sup>National Chemical Laboratory, Pune 411 008, India

MS received 25 July 2006; revised 28 August 2006

**Abstract.** Barium strontium titanate ((Ba<sub>0.87</sub>Sr<sub>0.13</sub>)TiO<sub>3</sub>–BST) ceramic powder was prepared by mechano-chemical process. The thick films of different thicknesses of BST were prepared by screen-printing technique and gas-sensing performance of these films was tested for various gases. The films showed highest response and selectivity to ammonia gas. The effect of film thickness on gas response was also studied. As prepared BST thick films were surface modified by dipping them into an aqueous solution of titanium chloride (TiCl<sub>3</sub>) for different intervals of time. Surface modification shifted response to H<sub>2</sub>S gas suppressing the responses to ammonia and other gases. The surface modification, using dipping process, altered the adsorbate–adsorbent interactions, which gave the unusual sensitivity and selectivity effect. Sensitivity, selectivity, thermal stability, response and recovery time of the sensor were measured and presented.

**Keywords.** (Ba<sub>0.87</sub>Sr<sub>0.13</sub>)TiO<sub>3</sub> thick films; ammonia gas sensor; H<sub>2</sub>S gas sensor; sensitivity; selectivity.

### 1. Introduction

The first semiconductor oxide gas sensors were reported by Seiyama *et al* in 1962. Since then, there have been numerous studies on other oxide semiconductors such as SnO<sub>2</sub>, ZnO, In<sub>2</sub>O<sub>3</sub>, TiO<sub>2</sub>,  $\alpha$ -Fe<sub>2</sub>O<sub>3</sub>, HfO<sub>2</sub>, WO<sub>3</sub>, BaSnO<sub>3</sub> (Seiyama *et al* 1962; Yamazoe *et al* 1983; Kabayashi *et al* 1988; Tamaki *et al* 1990; Lampe *et al* 1995; Nakamura *et al* 1998; Tao and Tsai 2002; Cantalini 2004). Semiconductor oxide gas sensors are extensively studied in order to improve their sensing characteristics, i.e. sensitivity, selectivity, stability, and response rate, to various kinds of gases and to meet the increasing needs of sensors in complicated systems and under strict conditions (Seiyama *et al* 1962; Yamazoe *et al* 1983; Kabayashi *et al* 1988; Tamaki *et al* 1990; Lampe *et al* 1995; Nakamura *et al* 1998; Tao and Tsai 2002; Cantalini 2004).

Detection of ammonia (NH<sub>3</sub>) is required in many applications including leak-detection in air conditioning systems, sensing of trace amounts in air for environmental analysis (Groot 2004), breath analysis for medical diagnoses (Timmer 2004), animal housing (Groot 2004) and more. Generally, because it is toxic, it is required to be able to sense low levels of NH<sub>3</sub>, but it should also be sensitive to much higher levels. NH<sub>3</sub> gas is very corrosive, often causing

existing NH<sub>3</sub> sensors to suffer from drift and have short life times. There are many principles for measuring NH<sub>3</sub> described in the literature (Timmer *et al* 2005; Yamazoe 2005). The ammonia sensors that have been manufactured in the largest quantities are mostly based on SnO<sub>2</sub> sensors (Clifford and Tuma 1983; Huebner and Drost 1991; Srivastava *et al* 1994; Sberreglieri 1995; Imawan *et al* 2000; Zakrzewska 2001). These sensors are rugged and inexpensive.

A different approach to make selective metal–oxide gas sensor is by using metals or additives that enhance the chemisorptions of specific gases. WO<sub>3</sub> based sensing material is demonstrated to respond to NH<sub>3</sub> (Wang *et al* 2000; Xu *et al* 2000). Very low detection limits of 1 ppm for ammonia sensing has been reported using a WO<sub>3</sub> ammonia sensor with Au and MoO<sub>3</sub> additives. This sensor is operated at an elevated temperature of more than 400°C (Xu *et al* 2000). Most sensors have much higher detection limits. Normal detection of these sensors ranges from 1–1000 ppm (Aslam *et al* 1999; Xu *et al* 2000). Another type of widely used ammonia sensor, employing electrolyte solutions with diaphragm electrodes, has major limitations due to the cost of fabrication and its relatively poor sensitivity and selectivity. Similarly, Pd gate metal oxide semiconductor device is also sensitive to ammonia but it does not offer sufficient selectivity, because ammonia is indirectly detected by sensing the hydrogen after decomposition (Lundström *et al* 1975; Winquist *et al* 1983).

\*Author for correspondence (lapresearch@rediffmail.com)

The perovskite oxides ( $\text{ABO}_3$ ) were used as gas sensor materials for their stability in thermal and chemical atmospheres. In the last decade, perovskite oxide ceramics such as  $\text{BaTiO}_3$  (Ishihara *et al* 1995; Haueusler and Meyer 1996; Liao *et al* 2001; Tang *et al* 2003; Zhou *et al* 2003; Jain *et al* 2006) and  $(\text{Ba}, \text{Sr})\text{TiO}_3$  (Slunečko *et al* 1992; Holc *et al* 1995; Tan *et al* 1999; Chen *et al* 2000; Zhu *et al* 2000; Agarwal and Sharma 2002; Roy *et al* 2005) have generated a lot of interest for chemical sensors. Modifications in microstructure, processing parameters and also concentration of acceptor/donor dopant can vary the temperature coefficient of the resistance and conductivity of  $\text{ABO}_3$  oxides. Sensors based on  $\text{ABO}_3$ -type complex oxide material, of rare earth elements have an outstanding merit of their sensitivity and better selectivity. These characteristics can be controlled by selecting suitable A and B atoms or chemically doping A' and B' elements equivalent, respectively to A and B into  $\text{ABO}_3$  to obtain  $\text{A}_x\text{A}'_{1-x}\text{B}_y\text{B}'_{1-y}\text{O}_3$  compound (Yan *et al* 1991; Kong and Shen 1996).

Gas sensing performance of screen-printed  $(\text{Ba}_{0.87}\text{Sr}_{0.13})\text{TiO}_3$  (BST) thick films is studied here. Jain and Patil (2006) studied the sensing behaviour of pure and modified  $(\text{Ba}_{0.67}\text{Sr}_{0.33})\text{TiO}_3$ , and reported that unmodified and modified  $(\text{Ba}_{0.67}\text{Sr}_{0.33})\text{TiO}_3$  are sensitive to  $\text{H}_2\text{S}$  gas. Here we report the effect of change in composition of BST, and on the sensing performance of  $(\text{Ba}_{0.87}\text{Sr}_{0.13})\text{TiO}_3$  and  $\text{TiO}_2$ -modified  $(\text{Ba}_{0.87}\text{Sr}_{0.13})\text{TiO}_3$ . In the present study, it was observed that response to  $\text{NH}_3$  gas increases with increase in  $(\text{Ba}_{0.87}\text{Sr}_{0.13})\text{TiO}_3$  film thickness up to certain limit, beyond that response decreases on further increase in thickness. However, Roy *et al* (2005) reported that the response to  $\text{NH}_3$  gas goes on increasing with film thickness. The sensitivity varied depending upon the thicknesses, microstructural variations, operating temperature and concentration of gas.  $(\text{Ba}_{0.87}\text{Sr}_{0.13})\text{TiO}_3$  thick films were surface modified using titanium chloride ( $\text{TiCl}_3$ ) solution by dipping technique. The surface modification shifts the sensitivity of  $(\text{Ba}_{0.87}\text{Sr}_{0.13})\text{TiO}_3$  thick film from  $\text{NH}_3$  to  $\text{H}_2\text{S}$  gas.

## 2. Experimental

### 2.1 Powder and paste preparation

AR grade powders of  $\text{Ba}(\text{OH})_2 \cdot 8\text{H}_2\text{O}$ ,  $\text{Sr}(\text{OH})_2$  with 7 : 1 molar concentration and  $\text{TiO}_2$  were milled for 2 h using planetary ball mill to obtain fine-grained powder. The powder was then calcined at  $1000^\circ\text{C}$  for 6 h.

The XRD spectrum of as prepared powder confirmed the sub-microcrystalline perovskite phase. The composition ratios (Ba/Sr) of the as prepared powder were confirmed using the microarea EDS analysis.

The BST powder was screen-printed using the procedure reported elsewhere (Jain and Patil 2006; Jain *et al* 2006)

onto a glass substrate in the desired pattern. The films were fired at  $550^\circ\text{C}$  for 30 min.

### 2.2 Preparation of surface modified BST thick films

The surface modified BST thick films were obtained by dipping them in a 0.1 M aqueous solution of titanium chloride ( $\text{TiCl}_3$ ) for different intervals of dipping time: 5, 10, 20 and 30 min. These films were dried at  $80^\circ\text{C}$ , followed by firing at  $550^\circ\text{C}$  for 30 min. These surface modified films are termed as ' $\text{TiO}_2$ -modified' films.

### 2.3 Variation of thickness

Films of various thicknesses were prepared by controlling the number of impressions of squeeze strokes. Different films of thicknesses: 1 BST ( $17\ \mu\text{m}$ ), 2 BST ( $33\ \mu\text{m}$ ), 3 BST ( $48\ \mu\text{m}$ ) and 4 BST ( $63\ \mu\text{m}$ ), were printed. The reproducibility in the thickness of the films was possible by maintaining proper rheology and thixotropy of the paste.

### 2.4 Characterization

The structural properties of powder were studied using RIGAKU model DMAX-2500 X-ray Diffractometer (XRD) with  $\text{CuK}\alpha$  radiation, having  $\lambda = 1.5406\ \text{\AA}$ . The microstructural and chemical compositions of the films were analysed using a scanning electron microscope (SEM, JEOL JED 6300) coupled with an energy dispersive spectrometer (EDS, JEOL JED 2300LA). The thickness of the thick films was measured using Taylor-Hobson (Talystep, UK) system. Thermogravimetric (TGA) analysis of the samples was carried out using a Mettler Toledo Star system-851 under similar conditions in static air. The sensing performance of the sensors was examined using a 'static gas sensing system' explained elsewhere (Jain and Patil 2006; Jain *et al* 2006).

## 3. Results and discussion

### 3.1 Structural properties

Figure 1 shows the X-ray diffractogram of screen-printed BST thick films fired at  $550^\circ\text{C}$  in air atmosphere.

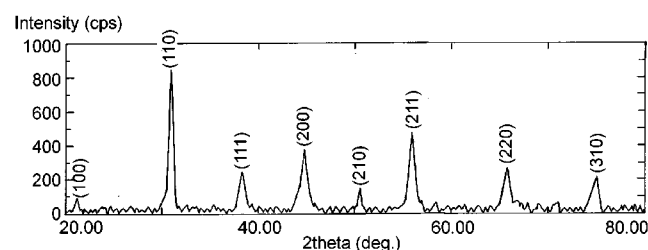


**Figure 1.** X-ray diffractogram of the BST thick films.

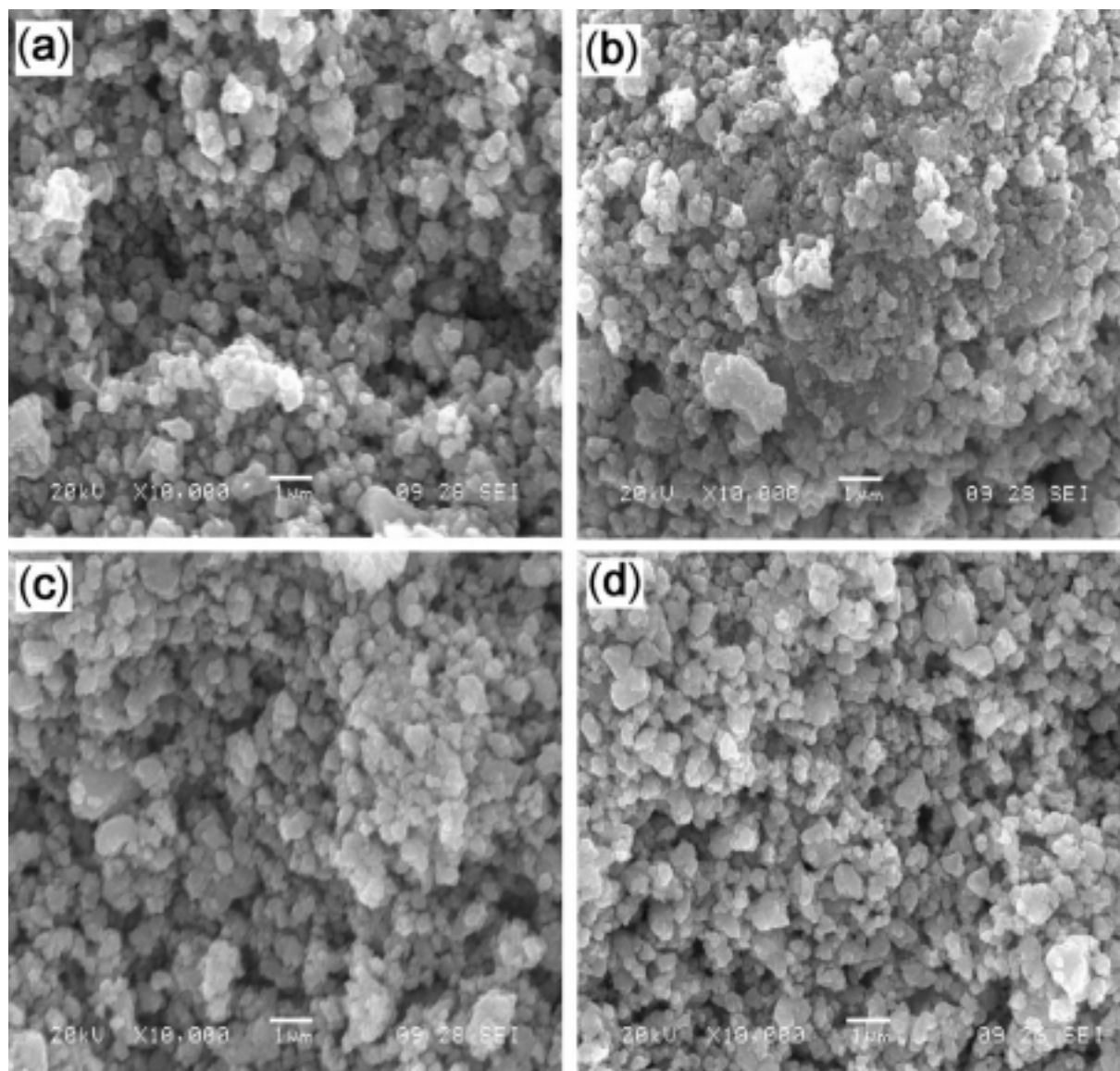


**Figure 2.** SEM images (a) unmodified 2 BST (33  $\mu\text{m}$ ), (b) unmodified 4 BST (63  $\mu\text{m}$ ), (c)  $\text{TiO}_2$ -modified 2 BST (dipped for 5 min), and (d)  $\text{TiO}_2$ -modified 2BST (dipped for 20 min).

XRD analysis revealed that the material is polycrystalline in nature with tetragonal perovskite phases. The peak positions matched well with the ASTM data book, card no. 34-11 and the average grain size determined from Scherrer formula is estimated to be 264 nm.

### 3.2 Microstructural analysis

Figure 2(a) depicts SEM image of unmodified 2 BST (33  $\mu\text{m}$ ) thick film fired at 550°C. The film consists of a large number of grains leading to high porosity and large effective surface area available for the adsorption of oxygen species. Figure 2(b) is the SEM image of the unmodified

4 BST film having larger thickness (63  $\mu\text{m}$ ). It is clear from the figure that it is comparatively less porous and grains are agglomerated. Effective surface to volume ratio would be decreased and less number of oxygen ions would be adsorbed as compared to the film in figure 2(a). Figure 2(c) is the SEM image of a  $\text{TiO}_2$ -modified 2 BST (33  $\mu\text{m}$ ) film for the dipping time interval of 5 min. The micrograph appears to consist relatively of smaller number of small particles distributed around the larger BST particles. The small particles would be of  $\text{TiO}_2$ . Figure 2(d) is the SEM image of a  $\text{TiO}_2$ -modified 2 BST (33  $\mu\text{m}$ ) film for the dipping time interval of 20 min. The micrograph appears to consist of a number of small particles distributed uniformly around the larger grains. The smaller particle may be at-

**Table 1.** Elemental analysis of unmodified and TiO<sub>2</sub>-modified BST films.

Element (wt%)	Dipping time (min)				
	0	5	10	20	30
(Ba + Sr + Ti)	93.16	93.23	93.33	93.86	92.86
Ti	00	0.22	0.30	0.43	0.64
O	6.84	6.55	6.37	5.71	6.50
BST	100	99.6323	99.4986	99.2813	98.9304
TiO <sub>2</sub>	00	0.3677	0.5014	0.7187	1.0696

tributed to the TiO<sub>2</sub> grains and the larger to BST. The film seems to be highly porous with a large effective area for oxygen adsorption.

### 3.3 Quantitative elemental analysis of unmodified and TiO<sub>2</sub>-modified BST films

The quantitative elemental composition of the film and wt.% of TiO<sub>2</sub> and BST analysed using an energy dispersive spectrometer are presented in table 1.

Stoichiometric (theoretically expected) wt% of cations (Ba + Sr + Ti) and anions (O) are 85.02 and 14.98, respectively. The wt% of constituent cations and anions in as prepared BST and TiO<sub>2</sub>-modified 2 BST were not as per the stoichiometric proportion and all samples were observed to be oxygen deficient, leading to the semiconducting nature of BST.

It is clear from table 1 that the weight percentage of TiO<sub>2</sub> increased with dipping time. The film with a dipping time of 20 min is observed to be more oxygen deficient (5.71 wt%). The observed oxygen deficiency was expected to promote increased oxygen adsorption.

### 3.4 Electrical conductivity

Figure 3 shows the dependence of conductivity of BST films with temperature in air and NH<sub>3</sub> ambient. Electrical conductivity of these films goes on increasing with increase in temperature in air and gas (NH<sub>3</sub>) ambient, indicating negative temperature coefficient (NTC) of resistance. This shows the semiconducting nature of the films. Slopes of the graphs between 50 and 300°C are different for different curves.

### 3.5 Thermal analysis

Figure 4 shows the thermogravimetric profile of pure and TiO<sub>2</sub>-modified 2 BST films. Table 2 lists the losses or gains in weight percentage of pure and TiO<sub>2</sub>-modified 2BST films in different ranges of temperature as observed from TGA. Comparatively a less weight loss and a more gain in the TiO<sub>2</sub>-modified 2 BST sample can be attributed to the

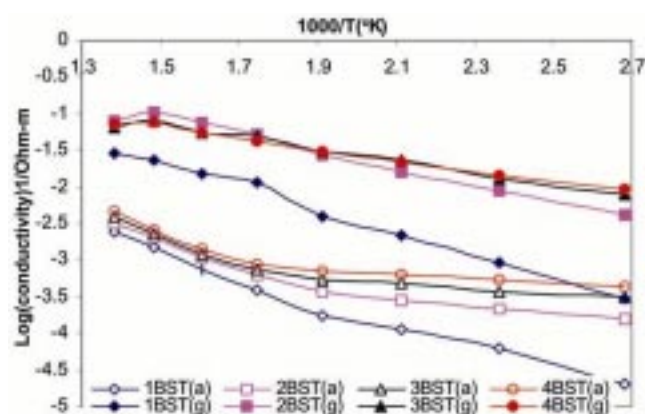


**Figure 3.** Variation of conductivity with operating temperature.

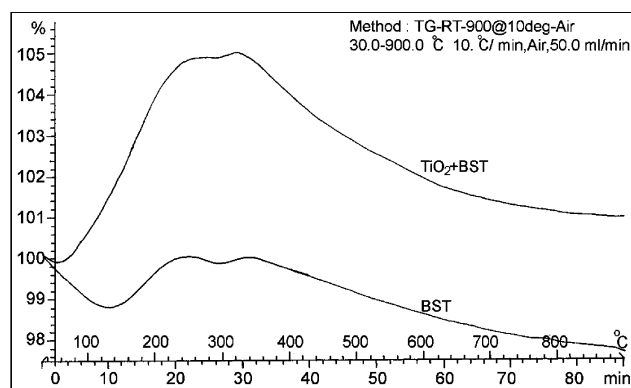


**Figure 4.** TGA of pure and TiO<sub>2</sub>-modified 2BST films.

adsorbed oxygen content. The film with TiO<sub>2</sub> content of 0.7187 wt% was observed to contain the smallest amount of oxygen (5.71 wt%, table 1), which could be attributed to the largest deficiency of oxygen in the film. It is, therefore, quite possible that the material would adsorb the largest possible amount of oxygen, showing a relatively larger gain in weight (5 wt%) in the temperature range 30–320°C. The TiO<sub>2</sub> on the surface of modified sample would form misfit regions between the grains of BST and could act as an efficient catalyst for oxygenation.

**Table 2.** Thermal analysis.

Temperature (°C)	Pure 2BST		Temperature (°C)	TiO <sub>2</sub> -modified 2BST	
	Loss (wt.%)	Gain (wt.%)		Loss (wt.%)	Gain (wt.%)
30–25	1.20	–	30–320	–	5.0
125–245	–	1.20	320–900	4.0	–
245–290	0.20	–			
290–340	–	0.20			
340–900	2.25	–			

## 4. Sensing performance

### 4.1 Sensing characteristics

Sensitivity is defined as the ratio of change in conductance of the sample on exposure to gas to the conductance in air.

$$S = \frac{Gg - Ga}{Ga} = \frac{\Delta G}{Ga},$$

where  $Gg$  and  $Ga$  are the conductances of the sample in the presence and absence of the test gas, respectively and  $\Delta G$  the change in conductance.

The ability of a sensor to respond to certain gas in the presence of other gases is known as selectivity. The time taken for the sensor to attain 90% of maximum change in resistance on exposure to gas is the response time. The time taken by the sensor to get back 90% of the original resistance is the recovery time (Ishihara *et al* 1991).

### 4.2 Unmodified BST films

**4.2a Sensitivity with operating temperature:** Figure 5 shows the variation in the sensitivity to NH<sub>3</sub> gas (300 ppm) with operating temperatures (for films of various thickness). It is noted from the graph that response increases with increasing temperature, and attains a maximum at 300°C, and decreases with further increase in operating temperature for all thicknesses and a film thickness of 33 μm is found to be most sensitive for sensing NH<sub>3</sub> gas.

**4.2b Variation of sensitivity with film thickness:** Figure 6 shows the variation in the sensitivity with film thickness, and the sudden change in sensitivity at a particular thickness could be related to the porosity in the screen-printed film. The porosity appears to increase with increasing film thickness. Beyond a certain thickness limit the porosity may decrease due to increase in agglomeration. The increased porosity increases the in-pore adsorption of oxygen and tends to improve the adsorption–desorption mechanism of target gas.

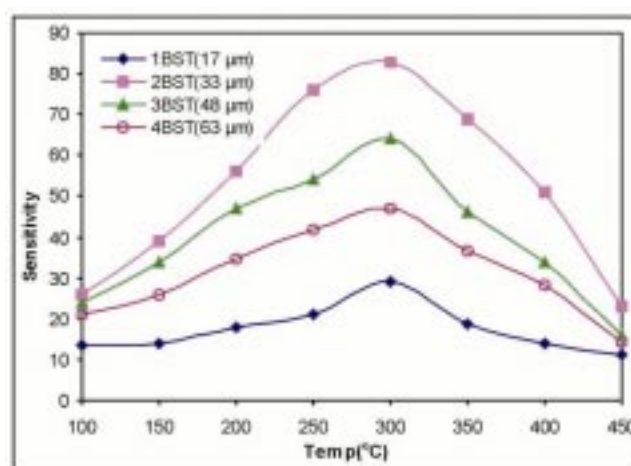


**Figure 5.** Variation of sensitivity with operating temperature for 300 ppm NH<sub>3</sub> gas.

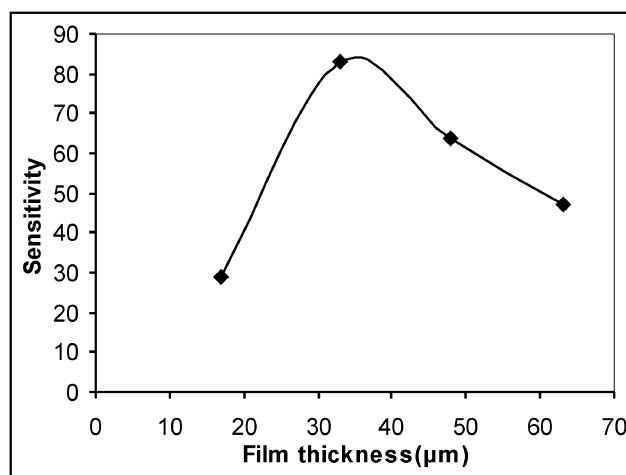


**Figure 6.** Variation of sensitivity to NH<sub>3</sub> gas with film thickness.

### 4.3 Response and recovery at different gas concentrations

Figure 7 shows the response and recovery profiles of the most sensitive unmodified (2BST) film to ammonia gas

at 300°C and it is observed that the response and recovery times increase as gas concentration increases.

Table 3 shows the values of response and recovery times at different gas concentrations. It is revealed that for lower gas concentration the response and recovery times are observed to be shorter, and become longer as gas concentration increases. Smaller the gas concentration faster would be the oxidation of NH<sub>3</sub> gas and hence quick response and immediate recovery of the sensor are noted.

4.4 TiO<sub>2</sub>-modified 2 BST films

4.4a Sensitivity and dipping time: Figure 8 shows the variation in the sensitivity of TiO<sub>2</sub>-modified 2 BST films to H<sub>2</sub>S and NH<sub>3</sub> gas at an operating temperature of 300°C, for films that were treated for different intervals of time for modification. It is clear from the figure that the response to H<sub>2</sub>S gas goes on increasing with the increase of dipping time interval, and reaches a maximum at 20 min, then decreases with further increase in dipping time while response to NH<sub>3</sub> gas goes on decreasing with dipping time.

Unmodified sample is more sensitive to NH<sub>3</sub> while TiO<sub>2</sub>-modified sample is more sensitive to H<sub>2</sub>S. The shift in the sensitivity of the modified film to H<sub>2</sub>S gas could be attributed to surface modification. Surface modification

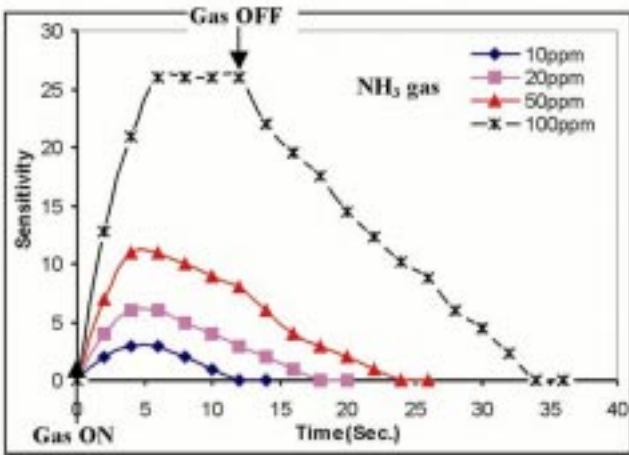


Figure 7. Response speed of the (2 BST) film at different NH<sub>3</sub> gas concentrations.

Table 3. Response and recovery times with gas concentrations.

Gas concentration (ppm)	Response time (s)	Recovery time (s)
10	3	10
20	4	16
50	5	20
100	6	32

would alter the adsorbate–adsorbent interactions and allows unusual selectivity and high sensitivity to H<sub>2</sub>S gas.

4.4b Sensitivity and operating temperature: Figure 9 compares the variation in the sensitivity of unmodified and TiO<sub>2</sub>-modified 2 BST films to H<sub>2</sub>S gas (300 ppm) with operating temperature. Unmodified samples showed weak response ( $S = 26$ ) to H<sub>2</sub>S gas at 350°C while TiO<sub>2</sub>-modified films (dipped for 20 min) showed maximum response ( $S = 114$ ) at 300°C. The surface modification enhanced the sensitivity to H<sub>2</sub>S gas and lowered the operating temperature as well.

4.5 Selectivity of pure and modified film

Figure 10 shows the histogram showing selectivities of unmodified and TiO<sub>2</sub>-modified 2 BST film. It is clear from the histogram that unmodified BST is more selective to NH<sub>3</sub> while TiO<sub>2</sub>-modified is more selective to H<sub>2</sub>S gas.

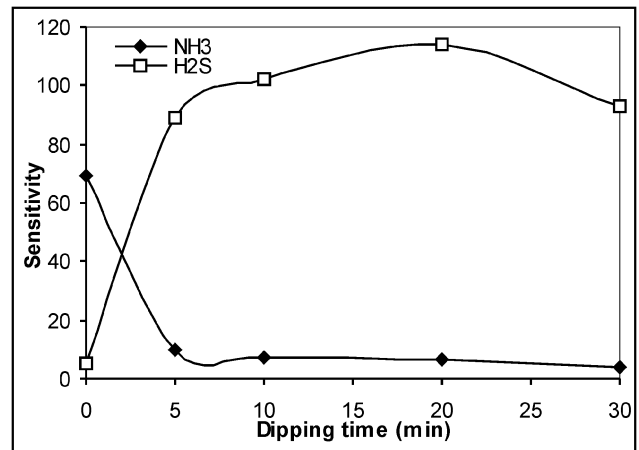


Figure 8. Variation of sensitivity to NH<sub>3</sub> and H<sub>2</sub>S gas with dipping time.

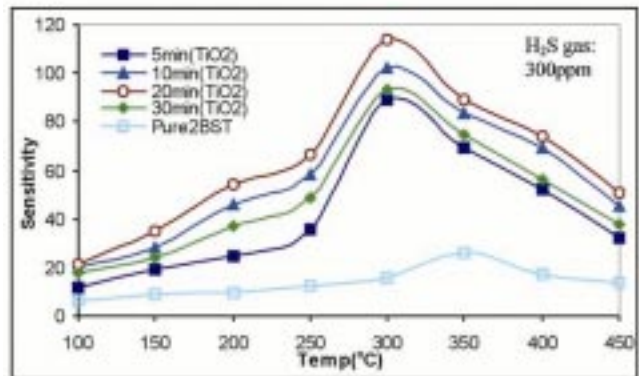


Figure 9. Comparison of sensitivity with unmodified and modified 2 BST films with temperature for H<sub>2</sub>S gas detection.

TiO<sub>2</sub> misfits on the surface of 2 BST film seem to be responsible for the shift in sensitivity from NH<sub>3</sub> to H<sub>2</sub>S gas.

#### 4.6 Response and recovery time of TiO<sub>2</sub>-modified film

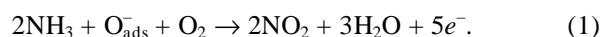
The response and recovery profiles for the most sensitive TiO<sub>2</sub>-modified 2BST film (20 min) are represented in figure 11. The response was quick (5 s) and the recovery time was 20 s, at 300°C to H<sub>2</sub>S gas for 30 ppm gas concentration.

### 5. Discussion

#### 5.1 BST as a NH<sub>3</sub> sensor

The sensitivity of (Ba<sub>0.87</sub>Sr<sub>0.13</sub>)TiO<sub>3</sub> to NH<sub>3</sub> could be attributed to the high oxygen deficiency and defect density and leads to increased oxygen adsorption. Larger the amount of oxygen adsorbed on the surface, larger would be the oxidizing capability and faster would be the oxidation of NH<sub>3</sub> gas. The reactivity of NH<sub>3</sub> would have been very large as compared to H<sub>2</sub>S gas with the surface under same condition. Hydrite (NH<sub>3</sub>) may have lower sensitivity than hydrogen exposed on particular metal oxide under same condition (Windichamann and Mark 1979). The lower response to NH<sub>3</sub> may be related to firm binding

state preventing fast decomposition and water formation. NH<sub>3</sub> could dissociate under certain favourable circumstances into (NH<sub>2</sub>)<sup>-</sup> and H<sup>+</sup> irreversibly. The reaction of released hydrogen with adsorbed or lattice oxygen could increase the conductance leading to higher sensitivity to NH<sub>3</sub>. NH<sub>3</sub> undergoes following reaction on exposure to metal surface:



Equation (1) represents the chemical reaction involved in unmodified BST to sense NH<sub>3</sub> gas. NH<sub>3</sub> molecule has a lone pair of electrons. In comparison with other gases, NH<sub>3</sub> can readily donate the unpaired electrons to the metal ions (of base material), which has unfilled orbits to form coordination complex. Furthermore, the coordinated NH<sub>3</sub> molecules easily react with oxygen adsorbates (O<sub>ads</sub><sup>-</sup>) and the electrons bonded with adsorbed oxygen are returned back into the sensor, increasing the sensor conductivity.

The adsorbed oxygen on the surface of catalyst can be of several forms: O<sub>2</sub>, O<sub>2</sub><sup>-</sup>, O<sup>-</sup> and O<sup>2-</sup>. Of these species, O<sub>2</sub> is quite inactive because it is in very low concentration. If reducing agent is introduced, the O<sup>-</sup> disappears very quickly relative to O<sub>2</sub><sup>-</sup> indicating the O<sup>-</sup> to be more active than O<sub>2</sub><sup>-</sup>. The lattice oxygen, O<sup>2-</sup>, can also be reactive with the incoming reducing agent.

#### 5.2 TiO<sub>2</sub>-modified BST as H<sub>2</sub>S gas sensor

In presence of reducing agent, solids are known to give up lattice oxygen (be reduced-ion exchange) and in presence of oxygen they become oxidized. This semiconductor could be used as gas sensors on redox principle. The ion exchange between a gas and a semiconductor could have a strong influence on the conductivity of the semiconductor. WO<sub>3</sub> has been reported (Roy Morrison 1982) to be completely converted to WS<sub>2</sub> by a few torr of H<sub>2</sub>S resulting in increase in conductivity.

Ion exchange mechanism between TiO<sub>2</sub> and H<sub>2</sub>S gas would be the reason behind the change in conductance. When H<sub>2</sub>S gas is exposed on TiO<sub>2</sub> modified BST film surface, the strong affinity of sulphur (electronegativity =

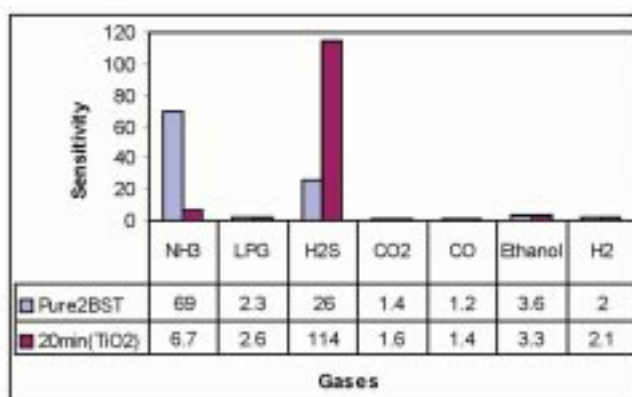


**Figure 10.** Selectivity of pure and TiO<sub>2</sub>-modified (20 min) 2 BST film.

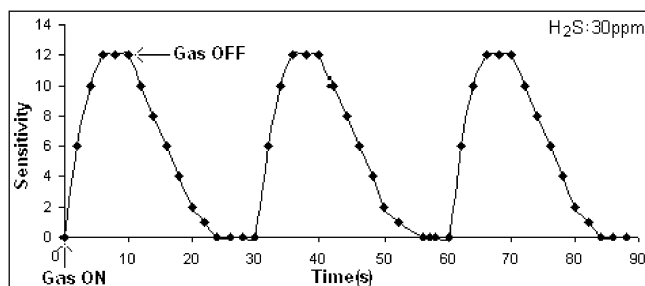


**Figure 11.** Response and recovery of the TiO<sub>2</sub>-modified 2 BST film.

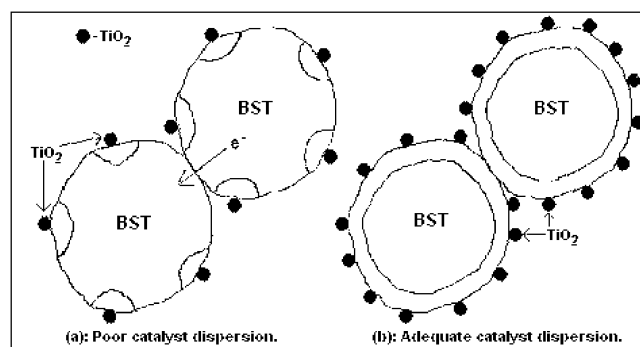


**Figure 12.** Dispersion of additive.

2.44) to the Ti atoms weakens the sulphur–hydrogen bond and facilitates dissociation to an  $S^{2-}$  or an  $SH^-$  ion and two or one  $H^+$  ions,  $TiO_2$  would be converted into well conducting  $TiS_2$ .

It is well known that additive lowers the activation energy of the reaction. The lowering of the activation energy can be described by simple illustrations:



and



Ion exchange in (2) requires little energy.  $H_2S$  could easily be dissociated in presence of  $TiO_2$ . To dissociate  $H_2S$  in absence of  $TiO_2$  would require large energy input. Larger the dissociation energy larger would be the activation energy. The activation energy required to dissociate  $H_2S$  would be to a great extent removed (lowered) by using  $TiO_2$  misfits as activator.

### 5.3 Effect of dipping time on $TiO_2$ dispersion and sensitivity

Figure 12 illustrates the effect of dispersion of surface additive on the film conductivity. Uniform and optimum dispersion of an additive dominates the depletion of electrons from semiconductor. Oxygen adsorbing on additive (misfit) removes electrons from additive and additive in turn removes electrons from the nearby surface region of the semiconductor and could control the conductivity.

For optimum dipping time (20 min), the number of  $TiO_2$  misfits would be optimum and would disperse uniformly covering the complete film surface (figure 12(a)). Adequate dispersion of  $TiO_2$  misfits (20 min) on film surface would produce depletion region on the grain surfaces and conductivity could be monitored systematically. The film conductivity would be very low in air and very high on exposure of  $H_2S$  gas (due to conversion of  $TiO_2$  into  $TiS_2$ ) and therefore, the sensitivity would be largest.

For the dipping time smaller than the optimum, the number of  $TiO_2$  misfits would be smaller, their dispersion would be poor and the depletion regions would be discontinuous and there would be the paths to pass electrons from one grain to another (figure 12(b)). Due to this, the initial conductance (air) would be relatively larger and in turn, sensitivity would be smaller.

For the dipping time larger than the optimum, the number of  $TiO_2$  misfits would be larger. This would mask and resist the gas to reach the base material (BST) giving lower sensitivity.

## 6. Conclusions

(I) The unmodified 2BST film is selective to  $NH_3$  sensor at  $350^\circ C$ .

(II) Sensitivity to  $NH_3$  gas increases with increase in film thickness and attains a maximum for  $33 \mu m$  and sensitivity decreases on further increase in thickness.

(III) Unmodified BST thick films were surface modified ( $TiO_2$ -modified) using dipping technique.

(IV)  $TiO_2$ -modified BST sensor is selective to  $H_2S$  gas suppressing the responses to other gases.

(V) Sensing properties of a particular material could be altered by surface modification.

## Acknowledgements

Authors are grateful to the Principal, Pratap College, Amalner, for providing laboratory facilities. Authors are grateful to Dr P K Khanna, C-MET, Pune, and Dr Dharmadhikari, Department of Physics, University of Pune, Pune, for their valuable cooperation rendered for the characterization of the material.

## References

- Agarwal S and Sharma G L 2002 *Sensors and Actuators* **B85** 205
- Aslam M, Choudhary V A, Mulla I S, Sainkar S R, Mandale A B, Belhekar A A and Vijayamohan K 1999 *Sensors and Actuators* **A75** 162
- Cantalanì C 2004 *Sensors and Actuators* **B24** 1421
- Chen X F, Zhu W G and Tan O K 2000 *Mater. Sci. & Engg.* **B77** 177
- Clifford P K and Tuma D T 1983 *Sensors and Actuators* **3** 233
- Groot T T 2004 *Sense of contacts 6, Keynote* (Netherlands (ECN): Sensor Research at Energy Research Centre)
- Haeusler A and Meyer J-U 1996 *Sensors and Actuators* **B34** 388
- Holc J, Slunečko J and Hrovat M 1995 *Sensors and Actuators* **B26-27** 99
- Huebner H P and Drost S 1991 *Sensors and Actuators* **B4** 463
- Imawan C, Solzbacher F, Steffs H and Obermeier E 2000 *Sensors and Actuators* **B64** 193
- Ishihara T, Kometani K, Hashida M and Takita Y 1991 *J. Electrochem. Soc.* **138** 173
- Ishihara T, Kometani K, Nishi Y and Takita Y 1995 *Sensors and Actuators* **B28** 49
- Jain G H and Patil L A 2006 *Bull. Mater. Sci.* **29** 403
- Jain G H, Patil L A, Wagh M S, Patil D R, Patil S A and Amalnerkar D P 2006 *Sensors and Actuators* **B117** 159
- Kabayashi T, Haruta M, Sano H and Nakane M 1988 *Sensors and Actuators* **13** 339
- Kong L and Shen Y 1996 *Sensors and Actuators* **B30** 217
- Lampe U, Gerblinger J and Meixner H 1995 *Sensors and Actuators* **B25** 657
- Liao B, Wei Q, Wang K Y and Liu Y X 2001 *Sensors and Actuators* **B80** 208
- Lundström I, Shivaraman M S and Svensson C M 1975 *J. Appl. Phys.* **46** 3876
- Nakamura Y, Zhang H, Kishimoto A, Okada O and Yanagida H 1998 *J. Electrochem. Soc.* **145** 632
- Roy Morrison S 1982 *Sensors and Actuators* **2** 329

- Roy S C, Sharma G L, Bhatnagar M C and Samanta S B 2005 *Sensors and Actuators* **B110** 299
- Sberreglieri G 1995 *Sensors and Actuators* **B23** 103
- Seiyama T, Kato A, Fujiishi K and Nagatani M 1962 *Anal. Chem.* **34** 1502
- Slunečko J, Holc J, Hrovat M and Čeh M 1992 *Sensors and Actuators* **B7** 439
- Srivastava R K, Lal P, Dwivedi R and Srivastava S K 1994 *Sensors and Actuators* **B21** 213
- Tamaki J, Maekawa T, Matsushima S, Miura N and Yamazoe N 1990 *Chem. Lett.* **19** 477
- Tan O K, Zhu W, Tse M S and Yao X 1999 *Mater. Sci. & Engg.* **B58** 221
- Tang Z -T, Zhou Z -G and Zhang Z -T 2003 *Sensors and Actuators* **B93** 391
- Tao W -H and Tsai C -H 2002 *Sensors and Actuators* **B81** 237
- Timmer B H 2004 *Amino-chip*, Ph D Thesis, U. Twente, The Netherlands
- Timmer B, Olthus W and Berg A V 2005 *Sensors and Actuators* **B107** 666
- Wang X, Miura N and Yamazoe N 2000 *Sensors and Actuators* **B66** 74
- Windichamann H and Mark P 1979 *J. Electrochem. Soc.* **126** 627
- Winqvist A, Spetz M, Armgarth C, Nylander C and Lundström I 1983 *Appl. Phys. Lett.* **43** 839
- Xu C N, Miura N, Ishida Y, Matuda K and Yamazoe N 2000 *Sensors and Actuators* **B65** 163
- Yamazoe N 2005 *Sensors and Actuators* **B108** 2
- Yamazoe N, Kurokawa Y and Seiyama T 1983 *Sensors and Actuators* **4** 283
- Yan W, Sun L, Lui M and Li W 1991 *Acta Scientiarum Naturalium Universitatis Jilinesis* **2** 52
- Zakrzewska K 2001 *Thin Solid Films* **391** 229
- Zhou Z -G, Tang Z -L and Zhang Z -T 2003 *Sensors and Actuators* **B93** 356
- Zhu W, Tan O K, Yan Q and Oh J T 2000 *Sensors and Actuators* **B65** 366